ARTICLE IN PRESS

Applied Thermal Engineering ■■ (2016) ■■–■■

Contents lists available at ScienceDirect

Applied Thermal Engineering

journal homepage: www.elsevier.com/locate/apthermeng

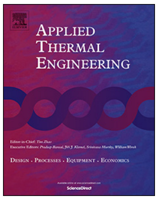

Research Paper

Analysis of industrial-scale high-temperature combined sensible/latent thermal energy storage

L. Geissbühler [a], M. Kolman [a], G. Zanganeh [b], A. Haselbacher [a,*], A. Steinfeld [a]

[a] *Department of Mechanical and Process Engineering, ETH Zurich, 8092 Zurich, Switzerland*
[b] *Airlight Energy Manufacturing SA, Via Industria 10, 6710 Biasca, Switzerland*

ARTICLE INFO

Article history:
Received 31 August 2015
Accepted 11 December 2015
Available online

Keywords:
Thermal energy storage
Packed bed
Phase change material
Exergy analysis
Simulation

ABSTRACT

An experimental-numerical approach was used to study combined sensible/latent heat storage based on placing a limited amount of steel-encapsulated $AlSi_{12}$ on top of a packed bed of rocks. The primary motivation for combining sensible and latent heat storage is to reduce the drop in outflow temperature during discharging that can be observed for sensible heat storage. An unsteady one-dimensional heat-transfer model was verified using exact solutions and validated with experimental data from a 42 kWh_{th} laboratory-scale combined storage. Simulations were then used to compare the performance of 23 MWh_{th} and 1000 MWh_{th} industrial-scale combined and sensible storages. The simulations showed that the combined storage can reduce the material costs for a given maximum outflow temperature drop during discharging. The simulations also demonstrated that the industrial-scale combined storages meet the goals of the U.S. Department of Energy's SunShot Initiative of exergy efficiencies greater than 95% and material costs below \$15/kWh_{th}.

1. Introduction

The integration of thermal energy storage (TES) improves the efficiency and economics of concentrated solar power (CSP) plants [1]. A thermocline TES based on a packed bed of rocks as sensible heat storage material and air as heat transfer fluid (HTF) is well-suited for CSP plants, yielding 95% overall (charging–discharging) thermal efficiency [2–4]. However, unless the storage is oversized, sensible heat thermocline systems suffer from decreases in the HTF outflow temperature during discharging, reducing the efficiency of the power block. Obviously, oversizing the storage increases costs and is therefore undesirable.

In principle, temperature decreases during discharging can be avoided with packed beds of encapsulated phase-change materials (PCMs). Several studies have concluded that packed beds composed of a single PCM do not offer clear benefits [5–7], however. Cascaded latent heat storage [8,9] appears promising, but requires additional experimental and numerical investigation. In particular, further research into characterization, phase-segregation and subcooling, compatibility of phase-change and encapsulation materials [10], cycling performance, and heat-transfer enhancement [11] are needed, especially at the high temperatures required for CSP [12,13].

These considerations prompt the investigation of combined sensible/latent-heat storage [14–18]. In prior work, such a combined storage was investigated numerically and experimentally at the laboratory scale. Placing 5% by volume of encapsulated $AlSi_{12}$ on top of a packed bed of rocks was found to be sufficient to stabilize the outflow temperature for approximately 90 minutes during discharging [16,17]. This allows a combined storage to be smaller than a sensible storage for the same temperature drop during discharging. The associated reduction in material offsets at least partially the increased cost of the PCM compared to the rocks. To the authors' knowledge, this offset has not been studied so far. The study of this offset is particularly relevant for industrial-scale TES where reduced material costs are an important contribution to lowering the levelized cost of the electricity produced by CSP plants [19].

Therefore, the objective of this article is to compare industrial-scale sensible and combined storage in terms of the exergy efficiency and specific material costs for a specified temperature drop of the HTF during discharging. Using the temperature drop during discharging as the basis for comparison is natural because the temperature of the HTF entering the power block has a direct impact on the efficiency of the power block. The comparison is based on a numerical model that is verified with exact solutions and validated with experimental data from a laboratory-scale combined storage.

2. Mathematical model

The quasi-one-dimensional heat-transfer model is based on the model developed by Zanganeh et al. [16] and formulated separately for the sensible and latent heat sections. Convective, conductive,

---

[*] Corresponding author. Tel.: +41 (0)44 632 69 05; fax: +41 (0)44 632 18 36.
E-mail address: haselbac@ethz.ch (A. Haselbacher).

http://dx.doi.org/10.1016/j.applthermaleng.2015.12.031
1359-4311/© 2015 Elsevier Ltd. All rights reserved.

Please cite this article in press as: L. Geissbühler, M. Kolman, G. Zanganeh, A. Haselbacher, A. Steinfeld, Analysis of industrial-scale high-temperature combined sensible/latent thermal energy storage, Applied Thermal Engineering (2016), doi: 10.1016/j.applthermaleng.2015.12.031

and radiative heat transfer are included and losses through the top, bottom, and circumferential walls of the storage are accounted for. The model described below improves that presented by Reference 16 by including the thermal inertia of the wall structure and insulation and the heat conduction in the encapsulated PCM.

2.1. Sensible heat section

The conservation equations for the fluid and solid phases are

$$(1-\phi_s)\frac{\partial(\rho_g e_g)}{\partial t}+(1-\phi_s)\frac{\partial(u\rho_g h_g)}{\partial x} = h_{v,\mathrm{rocks}}(T_s-T_g)+q_{\mathrm{loss,cover}}+q_{\mathrm{loss,bottom}}+a_w h_{w,\mathrm{conv}}(T_w-T_g), \quad (1)$$

$$\phi_s\frac{\partial(\rho_s e_s)}{\partial t}=\frac{\partial}{\partial x}\left(k_{\mathrm{eff}}\frac{\partial T_s}{\partial x}\right)+h_{v,\mathrm{rocks}}(T_g-T_s)+a_w h_{w,\mathrm{cond\text{-}rad}}(T_w-T_s), \quad (2)$$

where all symbols are defined in the nomenclature. Temperature-dependent rock and air properties are taken from References 3, 17, and 20. The volumetric heat-transfer coefficient $h_{v,\mathrm{rocks}}$ of the packed bed of rocks is determined from the correlation of Reference 21,

$$\mathrm{Nu}_{\mathrm{rocks}}=\frac{h_{\mathrm{rocks}}d_{\mathrm{rocks}}}{k_g}=\frac{2.06}{1-\varphi_s}\mathrm{Re}_{0,\mathrm{rocks}}^{0.425}\mathrm{Pr}_g^{1/3}\ [90\lesssim\mathrm{Re}_{0,\mathrm{rocks}}\lesssim 4000,\mathrm{Pr}_g\approx 0.7],$$

using

$$h_{v,\mathrm{rocks}}=\frac{6\phi_s}{d_{\mathrm{rocks}}}h_{\mathrm{rocks}}. \quad (3)$$

The Reynolds number $\mathrm{Re}_{0,\mathrm{rocks}}$ is based on the mean rock diameter d_{rocks} and the superficial velocity. For stagnant flow (during idle periods), the analytical Nusselt correlation for a sphere is used, $\mathrm{Nu}_{\mathrm{rocks}}=2$. The circumferential wall convective heat-transfer coefficient $h_{w,\mathrm{conv}}$ and the conductive-radiative wall heat-transfer coefficient $h_{w,\mathrm{cond\text{-}rad}}$ are taken from References 22 and 23, respectively. The effective thermal conductivity k_{eff} is calculated using the correlation of Reference 24, which is applied as described in Reference 3. The terms $q_{\mathrm{loss,cover}}$ and $q_{\mathrm{loss,bottom}}$ model the volumetric thermal losses from the top and bottom of the storage to the environment and are defined in Section 2.4.

The pressure drop in the packed bed is determined from Ergun's equation [25]. The sphericity of the packed-bed material is 0.6 for rocks and 1 for spheres. The case-dependent constants appearing in Ergun's equation are set to $A = 217$ and $B = 1.83$ for the rocks, as reported by Reference 26, where randomly shaped gravel of similar size and void fraction was used.

2.2. Latent heat section

Because PCMs can have low thermal conductivities, Biot numbers may be larger than 0.1. Therefore, the encapsulated PCM is discretized in the radial direction to account for thermal conduction inside the PCM. Spherical and cylindrical encapsulations are considered. Temperature-dependent PCM and encapsulation properties are given in Section 5.1.

2.2.1. Fluid

For the fluid phase, the energy conservation equation is

$$(1-\phi_{\mathrm{epcm}})\frac{\partial(\rho_g e_g)}{\partial t}+(1-\phi_{\mathrm{epcm}})\frac{\partial(u\rho_g h_g)}{\partial x} = a_w h_{w,\mathrm{conv}}(T_w-T_g)+q_{\mathrm{enc},g}+q_{\mathrm{loss,cover}}+q_{\mathrm{loss,bottom}}, \quad (4)$$

where ϕ_{epcm} is the volume fraction of the encapsulated PCM and $q_{\mathrm{enc},g}$ accounts for the convective heat transfer between the gas and encapsulation and is specified in the next section. The pressure drop for spherical encapsulations is calculated from Ergun's equation using $A = 150$ and $B = 1.75$.

2.2.2. Encapsulation

The energy conservation equation for spherical encapsulations is

$$\phi_{\mathrm{enc}}\frac{\partial(\rho_{\mathrm{enc}}e_{\mathrm{enc}})}{\partial t}=\frac{\partial}{\partial x}\left(k_{\mathrm{eff,pcm}}\frac{\partial T_{\mathrm{enc}}}{\partial x}\right) + a_w h_{w,\mathrm{cond\text{-}rad}}(T_w-T_{\mathrm{enc}})-q_{\mathrm{enc},g}+q_{\mathrm{pcm,enc}}, \quad (5)$$

where ϕ_{enc} is the volume fraction of the encapsulation. The effective thermal conductivity $k_{\mathrm{eff,pcm}}$ for spherical encapsulations is calculated from Reference 24, applying the relation given by Reference 27,

$$\mathrm{Pe}_{\mathrm{enc,eff}}=\frac{\dot m'' c_{p,g}d_{\mathrm{enc}}}{k_{\mathrm{eff}}}=\frac{\mathrm{Pe}_{\mathrm{enc},g}}{0.5\mathrm{Pe}_{\mathrm{enc},g}+k_{\mathrm{eff,stg}}/k_g}, \quad (6)$$

where $k_{\mathrm{eff,stg}}$ is the stagnant bed effective thermal conductivity.

For cylindrical encapsulations,

$$\phi_{\mathrm{enc}}\frac{\partial(\rho_{\mathrm{enc}}e_{\mathrm{enc}})}{\partial t}=-q_{\mathrm{enc},g}+q_{\mathrm{cond,enc}}+q_{\mathrm{rad,enc}}+q_{\mathrm{pcm,enc}} + \frac{a_w f_{\mathrm{cont},w}k_{\mathrm{enc}}}{(r_{\mathrm{tank}}-t_{\mathrm{enc}})\ln[r_{\mathrm{tank}}/(r_{\mathrm{tank}}-t_{\mathrm{enc}})]}(T_w-T_{\mathrm{enc}}), \quad (7)$$

where $f_{\mathrm{cont,w}}=0.002$ is the estimated fraction of the circumferential tank area in physical contact with the tubes and $q_{\mathrm{enc},g}$ represents the volumetric heat transfer between the fluid phase and the encapsulation considering convective and conductive resistances.

The volumetric heat-transfer contributions are based on the cell volumes of the quasi-one-dimensional model. Therefore, it is necessary to introduce the subscript i to indicate the axial location in the grid associated with the model. For the cell with axial index i and volume V_i, the volumetric heat transfer between encapsulation and gas is given by $q_{\mathrm{enc},g,i}=(T_{\mathrm{enc},i}-T_{g,i})/V_i(R_{\mathrm{cond},i}+R_{\mathrm{conv},i})$. The conductive thermal resistances for spherical and cylindrical encapsulations are given by the standard expressions in which the number of spheres or tubes in cell i are taken into account. The conductive resistance is based on the mean length of the cylindrical tubes in a given row. For spherical encapsulations, $h_{v,\mathrm{enc},i}$ is calculated from Eq. (3) (appropriately modified) and from the correlation of Reference 28,

$$\mathrm{Nu}_{\mathrm{enc}}=\frac{h_{\mathrm{enc}}d_{\mathrm{enc}}}{k_g}=2.0+2.031\mathrm{Re}_{0,\mathrm{enc}}^{1/2}\mathrm{Pr}_g^{1/3} + 0.049\mathrm{Re}_{0,\mathrm{enc}}\mathrm{Pr}_g^{1/2}\quad[\mathrm{Re}_{0,\mathrm{enc}}<5000]. \quad (8)$$

For cylindrical encapsulations, $h_{v,\mathrm{enc},i}$ is determined from $h_{v,\mathrm{enc},i}=a_{s,i}h_{\mathrm{enc},i}$ with $a_{s,i}$ being the calculated surface area of the tubes divided by the total volume of the cell (including the volume of encapsulation, PCM, and gas) and the heat-transfer coefficient per unit area h_{enc} is calculated from the correlation of Reference 29,

$$\mathrm{Nu}_{\mathrm{enc}}=\frac{h_{\mathrm{enc}}d_{\mathrm{tubes}}}{k_g}=0.51C_{\mathrm{row}}\mathrm{Re}_{\mathrm{max}}^{1/2}\mathrm{Pr}_g^{0.37}\left(\frac{\mathrm{Pr}_g}{\mathrm{Pr}_s}\right)^{1/4} \quad [40<\mathrm{Re}_{\mathrm{max}}<1000],$$

where $C_{\mathrm{row}}=0.95$ (for four staggered tube rows as in the experimental setup described below), $\mathrm{Re}_{\mathrm{max}}$ is based on d_{tubes} and $u_{\mathrm{max}}=S_t u_0/(S_t-d_{\mathrm{tubes}})$ with S_t denoting the transversal pitch, Pr_g is the gas Prandtl number evaluated at the gas temperature, and Pr_s is the gas Prandtl number evaluated at the solid temperature.

Please cite this article in press as: L. Geissbühler, M. Kolman, G. Zanganeh, A. Haselbacher, A. Steinfeld, Analysis of industrial-scale high-temperature combined sensible/latent thermal energy storage, Applied Thermal Engineering (2016), doi: 10.1016/j.applthermaleng.2015.12.031